A novel intracellular pool of LFA-1 is critical for asymmetric CD8+ T cell activation and differentiation

Tara Capece, Brandon L. Walling, Kihong Lim, Kyun-Do Kim, Seyeon Bae, Hung-Li Chung, David J. Topham, and Minsoo Kim

Department of Microbiology and Immunology, David H. Smith Center for Vaccine Biology and Immunology, University of Rochester, Rochester, NY

The integrin lymphocyte function–associated antigen 1 (LFA-1; CD11a/CD18) is a key T cell adhesion receptor that mediates stable interactions with antigen-presenting cell (APC), as well as chemokine-mediated migration. Using our newly generated CD11a-mYFP knock-in mice, we discovered that naive CD8+ T cells reserve a significant intracellular pool of LFA-1 in the uropod during migration. Intracellular LFA-1 quickly translocated to the cell surface with antigenic stimulus. Importantly, the redistribution of intracellular LFA-1 at the contact with APC was maintained during cell division and led to an unequal inheritance of LFA-1 in divided T cells. The daughter CD8+ T cells with disparate LFA-1 expression showed different patterns of migration on ICAM-1, APC interactions, and tissue retention, as well as altered effector functions. In addition, we identified Rab27 as an important regulator of the intracellular LFA-1 translocation. Collectively, our data demonstrate that an intracellular pool of LFA-1 in naive CD8+ T cells plays a key role in T cell activation and differentiation.

Introduction

Naive T cells spend their lifespan circulating from the blood to lymphatic organs in search of cognate antigen presented by antigen-presenting cells (APCs) and then returning to the blood via the thoracic duct in a cyclical fashion. Successful expansion and differentiation of naive CD8+ T cells is dependent on the ability of cells to precisely localize with APCs in secondary lymphoid organs to form stable and prolonged interactions upon antigen recognition and T cell receptor (TCR) activation (Kaech et al., 2002; Cronin and Penninger, 2007; Chen and Flies, 2013). To undergo further T cell expansion and differentiation, T cells require additional stimuli from APCs and lymphatic cells that reside within niches in secondary lymphoid organs. Therefore, recirculation through lymph nodes, interactions with APCs, and localization to distinct immune niches are likely to impact CD8+ T cell division and differentiation. A key molecule regulating these processes is the integrin lymphocyte function–associated antigen 1 (LFA-1).

Adhesive force generated by LFA-1 ligation is essential for initial T cell entry into the lymph node through high endothelial venules (Weber et al., 2001) and subsequently T cell retention through interaction with the lymphatic stroma and APCs (Smith et al., 2003, 2007; Katakai et al., 2013). LFA-1 knockout (KO) T cells pass through the lymph node more rapidly and are three times more likely to exit (Reichardt et al., 2013). Enhanced LFA-1 adhesiveness is equally important for the maintenance of the immunological synapse and the signal integration necessary for complete T cell activation. Once a naive T cell encounters an antigen-bearing APC, LFA-1 engagement with ICAM-1 overcomes the glycocalyx repulsion of the T cell–APC contact and brings the two cells within a 40-nm proximity, allowing actin-mediated lamellipodia protrusion to sustain TCR signaling (Choudhuri et al., 2005). In addition to the physical adhesion, LFA-1 also provides important costimulation signals while excluding negative regulators of TCR signaling (Matsumoto et al., 2004; Graf et al., 2007).

Many signaling molecules have emerged as important players in regulating LFA-1 functions in T cells. Surface receptors, such as chemokine receptors or TCR, induce activation of downstream signaling molecules (Rap1 and talin) that leads to conformational changes in LFA-1 (Kim et al., 2003). Alternatively, outside-in signals occur when LFA-1 binds multivalent ICAM-1, stabilizing clusters of the active conformation and inducing downstream signals for cytokine production, proliferation, and survival (Salomon and Bluestone, 1998; Ni et al., 2001; Kandula and Abraham, 2004; Kim et al., 2004; Varga et al., 2010). In addition to receptor-induced activation, LFA-1 adhesiveness is also modulated by cell surface localization through lateral mobility (Cairo et al., 2006) and intracellular trafficking of important mediators of LFA-1 activation, including Rap1, Rap2, RapL, and Mst1, through Rab5, Rab11, Rab13, and EEA1 endosomes (Fabbri et al., 2005; Stanley et al., 2012; Svensson et al., 2012; Nishikimi et al., 2014). Although it has

Correspondence to Minsoo Kim: minsoo_kim@urmc.rochester.edu

Abbreviations used: APC, antigen-presenting cell; BMDC, bone marrow–derived cell; dpi, day post infection; hpi, hour post invasion; KI, knock-in; KO, knockout; LFA-1, lymphocyte function–associated antigen 1; MHC, major histocompatibility complex; MTOC, microtubule organizing center; TCR, T cell receptor.

The Rockefeller University Press
J. Cell Biol. Vol. 216 No. 11 3817–3829
https://doi.org/10.1083/jcb.201609072

been suggested that these vesicle cargos may contain LFA-1 (Hogg et al., 2011), dynamic regulation of LFA-1 redistribution during activation of naive T cells has yet to be demonstrated.

Dynamic regulation of LFA-1 expression and functions in T cells is typically studied using cell lines and/or activated T cell blasts with transfection of recombinant genes or monoclonal antibodies that detect cell surface expression. Given the importance of the dynamic LFA-1 regulation during naive T cell migration and activation, these approaches are not sufficient to completely understand LFA-1 biology. In this study, we generated CD11a-mYFP knock-in (KI) mice to study endogenous LFA-1 expression and distribution patterns. Using live imaging of fluorescence CD11a-mYFP in CD8$^+$ T cells from the newly developed KI mouse, we report a previously undescribed intracellular pool of LFA-1 that is critical for T cell activation and differentiation.

Results

Naive CD8$^+$ T cells possess an intracellular pool of LFA-1

The integrin LFA-1 (CD11a/CD18) is expressed on most leukocytes and plays a key role in regulating leukocyte adhesion, migration, and activation. To study dynamic regulation of endogenous LFA-1 expression during T cell activation and differentiation, we generated a KI mouse in which the α subunit of LFA-1 (CD11a) was fused with monomeric YFP (CD11a-mYFP; Fig. 1, A–D). Extensive characterization revealed that immune development (Fig. S1 A), LFA-1 function (Fig. S1, B and C), T cell activation (Fig. S1 D), and T cell effector function (Fig. S1 E) in CD11a-mYFP and WT mice were comparable.

To further confirm that the cellular expression of endogenous LFA-1 in CD11a-mYFP mice was comparable to that of WT mice, we investigated the distribution pattern of LFA-1 in naive CD8$^+$ T cells. First, CD11a-mYFP mice showed normal cell surface expression of LFA-1 on naive CD8$^+$ T cells compared with WT mice (Fig. S2 A). To our surprise, however, optical scanning (Fig. 1 E and Video 1) and flow cytometry analysis using two different cell-permeabilization methods (Fig. S2, B and C) of naive CD8$^+$ T cells from CD11a-mYFP/OT-I mice revealed a previously unrecognized intracellular pool of LFA-1. Intracellular LFA-1 was primarily concentrated to the uropod of migrating cells (Fig. 1 E, migration; and Video 2). Strikingly, time-lapse imaging of live naive CD8$^+$ T cells showed that the majority of intracellular LFA-1 in the uropod rapidly localized to the T cell and ovalbumin (OVA) (N4)-loaded APC contact site (Fig. 1 E, conjugation; and Video 3).

Intracellular LFA-1 redistributes to the cell membrane during T cell activation

To determine whether this rapid redistribution of intracellular LFA-1 was dependent on antigen affinity to the TCR, we stimulated naive CD8$^+$ T cells with N4 or a low-affinity altered peptide ligand (D7; Koniaras et al., 1999) that showed reduced T cell activation and proliferation (Fig. 2 A) but comparable stability on major histocompatibility complex (MHC) class I molecules and calcium flux (Fig. S3, A and B). Unlike activation with N4-bearing APCs, in which intracellular LFA-1 localized to the immunological synapse (Fig. 2, B and C; Fig. S3 C; and Video 3) and rapidly became available for cell–cell interactions on the T cell surface (Fig. 2, D and E), D7-bearing APCs failed to induce the rapid translocation of LFA-1 to the cell surface (Fig. 2, B–E; and Video 4).

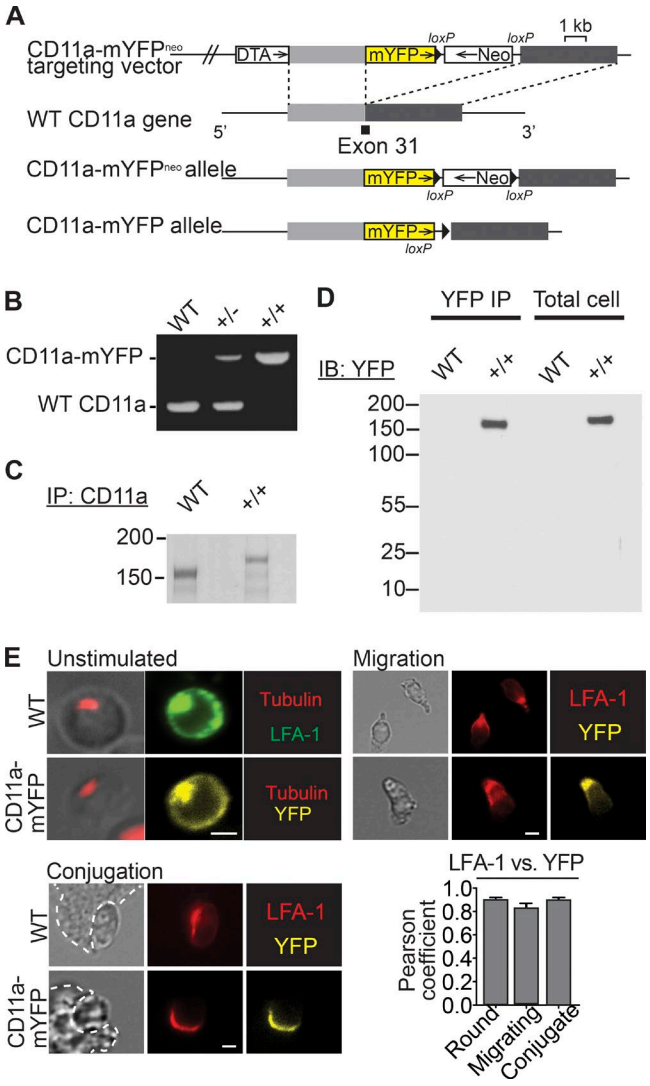

Figure 1. **Naive CD8$^+$ T cells possess an intracellular pool of LFA-1.** (A) Schematic of CD11a-mYFP mouse generation. The mYFP sequence was knocked into the C terminus of the mouse integrin CD11a subunit. (B) CD11a PCR depicting the increased size of CD11a corresponding with the mYFP tag. (C) Corresponding size increase was also detected in a silver stain at the protein level. mAb M17/4 was used for immunoprecipitation of CD11a. (D) Western blot analysis of YFP expression in YFP immunoprecipitate (IP) and total cell lysate from splenocytes of CD11a-mYFP mice showing the intact YFP conjugation to CD11a. No evidence of proteolytic cleavage of YFP was detected. (E) Representative images of permeabilized naive CD8$^+$ T cells stained with CD11a (LFA-1) or α-tubulin antibodies on noncoated glass surface (unstimulated/round), after 30 min of migration on ICAM-1 and CCL21 coating (migration) or after 60 min of conjugation with N4-pulsed BMDCs (conjugation) showing the intracellular pool of LFA-1. Bars, 2 µm. Graph shows colocalization of YFP signal versus anti–CD11a antibody (LFA-1) signal in naive CD11a-mYFP CD8$^+$ T cells. Pearson coefficient was generated as YFP (CD11a-mYFP)/red (anti-CD11a). Note that the YFP signal and the anti–CD11a antibody (LFA-1) signal are highly colocalized in naive CD11a-mYFP CD8$^+$ T cells. Data are presented as mean ± SEM; n = 4 mice/group (10–20 cells per mouse). Note that there are equivalent levels of total LFA-1 (intracellular staining and surface LFA-1) detected in both saponin and Triton X-100 permeabilized samples (Fig. S2 C).

We further confirmed the dynamic redistribution of intracellular LFA-1 to the cell surface during early T cell activation

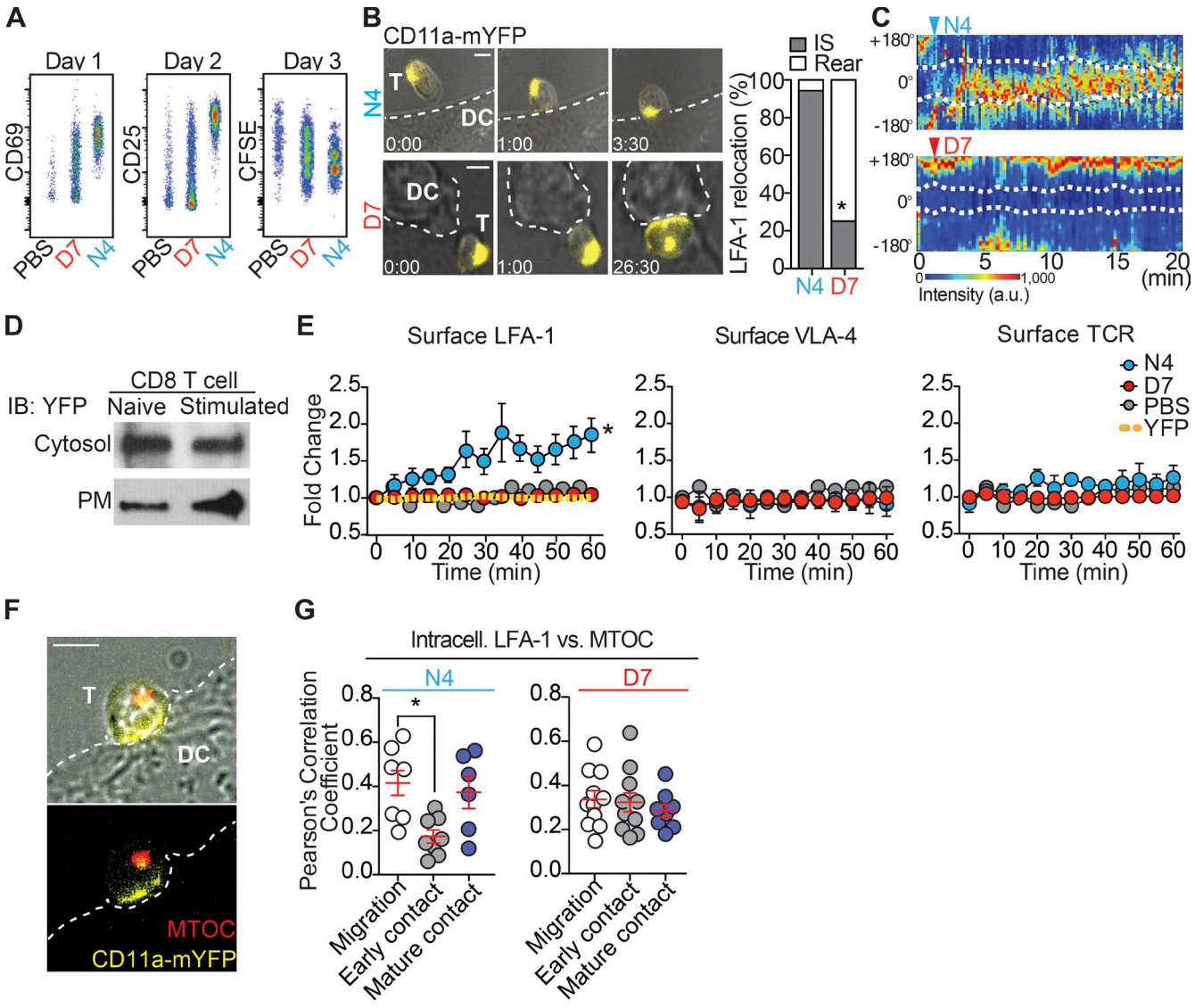

Figure 2. **Redistribution of intracellular LFA-1 during T cell activation.** (A) Representative flow cytometry analysis of T cell activation (CD69 and CD25) and proliferation (CFSE dilution) after stimulation of naive T cells with cognate ligand (N4) or altered peptide ligand (D7)–loaded irradiated splenocytes; $n = 4$ mice. (B) Representative images from real-time T cell contacts with APCs loaded with N4 or D7 peptide on plates coated with ICAM-1 and CCL21. Bars, 5 µm. In the graph, each bar represents the percentage of total cells scored after 45 min of co-culture. The gray portion of each bar is the fraction of cells exhibiting dominant YFP signal at the immunological synapse (IS) region, and the white portion is the fraction of the cells that showed YFP signal at the posterior region. Data represent mean ± SEM; $n = 3$ mice/group (30–42 cells per mouse). *, $P < 0.05$. (C) Representative fluorescence intensity of CD11a-mYFP cell surface from B. YFP fluorescence intensity is shown in a pseudocolor scale (from low [black] to high [red]). +/− 180°, rear of cell; 0°, leading edge; white lines depict the T cell–APC interface; arrowheads indicate the beginning of the T cell–APC contact. (D) Representative Western blot analysis of YFP expression in cell cytosol and plasma membrane (PM) fractions from naive CD11a-mYFP CD8$^+$ cells or cells stimulated with CD3/CD28 antibodies for 30 min. Note that CD11a-mYFP protein level was increased in PM after T cell activation. $n = 3$ mice. (E) Flow cytometry analysis of surface LFA-1, VLA-4, and TCR levels after indicated times of naive CD11a-mYFP/OT-I CD8$^+$ T cell and peptide-pulsed or PBS-treated BMDC co-culture. YFP$^+$ T cells were fixed at indicated times and stained for surface expression. Total LFA-1 levels measured by mYFP intensity (yellow line). Data normalized to PBS control. Data are expressed as mean ± SEM of six separate experiments. *, $P < 0.001$. (F) Representative image of naive CD11a-mYFP CD8$^+$ T cells stained with ER Tracker (MTOC; red) during N4-loaded APC interaction on the ICAM-1+CCL21–coated surface. Note that CD11a-mYFP and the MTOC are not colocalized during the LFA-1 redistribution. Bar, 5 µm. (G) The MTOC and CD11a-mYFP are colocalized during migration and mature APC contact, but not during early LFA-1 translocation to the APC contact ("early contact") when stimulated by N4. The Pearson's correlation coefficient was generated as YFP (LFA-1)/red (MTOC). Circles represent individual cells from three independent experiments with mean shown as a line. Data represent mean ± SEM. *, $P < 0.01$.

using flow cytometry analysis of naive CD8$^+$ T cell isolated from WT mice (Fig. S3 D). Furthermore, the integrin VLA-4 and TCR did not exhibit the same dynamic redistribution pattern as LFA-1, suggesting the presence of a specific redistribution pathway for LFA-1 (Fig. 2 E). Total CD11a-mYFP protein expression levels measured by YFP intensity remained constant during the T cell activation (Figs. 2 E and S3 E), and Exo1, an inhibitor of exocytosis of newly synthesized proteins, did not alter redistribution of LFA-1 (Fig. S3 F). Therefore, the results suggest that LFA-1 redistribution is not a consequence of de novo protein production. In addition, cells treated with Dynasore, a dynamin inhibitor that blocks a majority of endocytosis (Macia et al., 2006), exhibited similar intracellular and cell surface levels of LFA-1 as detected by flow cytometry, suggesting that endocytic recycling has minimum impact on intracellular LFA-1 in naive T cells (Fig. S3 G). Finally, we confirmed that LFA-1

redistribution was independent of relocalization of the microtubule organizing center (MTOC) to the immunological synapse (Fig. 2, F and G; and Fig. S3 H), antigen concentration (Fig. S3, I and J), and LFA-1–ligand interactions (Fig. S3, K and L).

To determine whether the intracellular LFA-1 redistribution found in early T cell activation is maintained through cell division during APC contacts, we imaged the dynamic division of CD11a-mYFP-expressing OT-I $CD8^+$ T cells in vitro. T cells and N4-loaded bone marrow–derived cells (BMDCs) were co-cultured on ICAM-1–coated plates for 30 h and imaged to capture T cell division. Live imaging of the T cell division while in contact with an APC demonstrated a pronounced polarized distribution of LFA-1 at the synapse that persisted throughout the initial cell division and resulted in the unequal partitioning of LFA-1 into the two daughter cells (YFP^{high} vs. YFP^{low}; Fig. 3 A and Video 5). In contrast, T cell division outside of APC contact led to equal distribution of LFA-1 into the two daughter cells (Fig. 3 B). Note that $CD8^+$ T cells engage in several APC contacts during activation and before their first division (Mempel et al., 2004; Eickhoff et al., 2015), and cell division can occur while T cells are with or without a physical contact with APCs. Flow cytometry analysis further demonstrated unequal partitioning of LFA-1 in vivo as detected by YFP intensity in CD11a-mYFP/OT-I $CD8^+$ T cells from mice infected with influenza virus x31-OVA (Fig. 3 C). Importantly, we also observed unequal partitioning of another known T cell immunological synapse marker, CD8, during T cell division, showing over 90% correlation of LFA-1^{high} with $CD8^{high}$ or LFA-1^{low} with $CD8^{low}$ (Figs. 3 C and S4). In addition to LFA-1, naive CD8 T cells express integrin VLA-4 (CD49d/CD29), which plays a key role in extravasation through high endothelial venules and intranodal migration, during which APC scanning occurs (Hyun et al., 2009). Furthermore, chemotactic molecules such as CCL21, CCL19, CXCL12, and S1p presented in the lymph node and their receptors, including CCR7, CXCR4, and S1PR, are essential for T cell migration and the signal integration necessary for complete T cell activation (von Andrian and Mackay, 2000; Pham et al., 2008). Although flow cytometry analysis clearly showed asymmetric expression of LFA-1 in first-division T cells, we did not observe disparate expression of other T cell surface molecules known to mediate T cell migration (Fig. 3 D).

Differential LFA-1 levels lead to changes in T cell migration and conjugation

To determine whether disparate LFA-1 expression in first-division $CD8^+$ T cells regulates the dynamic patterns of T cell migration and APC interactions during early T cell activation, we isolated YFP^{high} (LFA-1^{high}) and YFP^{low} (LFA-1^{low}) first-division $CD8^+$ T cells from influenza-infected mice (Fig. 3 C). In vitro migration assays on plates coated with ICAM-1 and CCL21 revealed two distinct cell migration patterns in the LFA-1^{high} and LFA-1^{low} T cells (Fig. 4 A). To evaluate T cell–APC conjugation patterns, OVA-pulsed BMDCs were first adhered to a chamber coated with ICAM-1 and CCL21. T cells were then placed in the chamber, and cell–cell interactions were imaged. The frequency of APC conjugation of LFA-1^{high} (YFP^{high}) versus LFA-1^{low} (YFP^{low}) $CD8^+$ T cells was measured. Among cells imaged, 75% of LFA-1^{high} T cells spent more than 70% of imaging time forming stable contacts with OVA-loaded APCs, whereas the majority (over 80%) of LFA-1^{low} T cells never or only transiently (less than 30% of imaging time) contacted APCs. Importantly, the majority of stopped T cells (>80%) productively engaged with APCs during their conjugation time as measured by calcium flux (Fig. S3 B). Thus, migration and APC interaction patterns in T cells with differential LFA-1 expression demonstrate that higher LFA-1 expression allows formation of stable and prolonged T cell–APC conjugates over time, whereas reduced LFA-1 expression permits a highly migratory state. Our data suggest unequal partitioning of LFA-1 during cell division generates daughter cells with differential behavior patterns, guiding T cell migration, interactions, and localization.

Different patterns of T cell behavior may lead to increased integration of signals required for differentiation versus further APC scanning, migration to other regions of the lymph node, or access to sites of egress. Thus, the exposure of first-division T cells to diverse immune niches could alter T cell differentiation programs by reinforcing or redefining existing environmental cues. To determine whether unequal LFA-1 inheritance affected T cell retention in the lymph node, we conducted a competitive egress assay. To evaluate the rate at which cells exit the lymph node, mice were treated with an antibody against CD62L to block entry of additional T cells 12 h before the first division. The number of T cells retained in the draining lymph node was compared with the number of T cells measured in mice treated with both the CD62L antibody and FTY720, an inhibitor of T cell egress (Matloubian et al., 2004). Flow cytometry analysis of T cell number in the draining lymph node and spleen revealed that when additional T cell entry was blocked by CD62L antibody, the first-division LFA-1^{low} T cell population was quickly egressed from the draining lymph node, whereas a larger number of LFA-1^{high} T cells remained in the inflamed lymph node for a longer period (Fig. 4 B). To determine whether the migration and retention of T cells in the draining lymph node resulted in cells receiving differential effector functions, we first measured the mRNA levels of the transcription factor T-bet and effector molecules interferon-γ and granzyme B (Kelso et al., 2002). LFA-1^{high} T cells isolated from influenza-infected mice exhibited higher expression of effector gene products than LFA-1^{low} T cells (Fig. 4 C). Second, we tested the ability of LFA-1^{high} and LFA-1^{low} $CD8^+$ T cells to generate memory cells after primary influenza infection. Upon infection of recipients with influenza virus X31-OVA, we found that both LFA-1^{high} and LFA-1^{low} cells expanded equally well in the lymph node and lung during the primary response (8 d post infection [dpi]; Fig. 4 D). However, the number of CD11a-$mYFP^+$ T cells in the lung 60 dpi was significantly reduced when LFA-1^{high} T cells were transferred before primary infection (Fig. 4 E). Furthermore, LFA-1^{high} T cells were unable form the central memory, effector memory, and tissue-resident memory compartments 60 dpi (Fig. 4 F). This result is in agreement with earlier studies demonstrating that $CD8^{low}$ cells, but not $CD8^{high}$ T cells, clear secondary infection (Chang et al., 2007; Ciocca et al., 2012). Collectively, these data demonstrate that LFA-1^{high} and LFA-1^{low} $CD8^+$ T cells exhibit distinct migration, T cell–APC interaction, and lymph node retention patterns that generate unique differentiation programs.

Rab27 mediates redistribution of intracellular LFA-1 during naive $CD8^+$ T cell activation

Several molecules are known to asymmetrically partition into first-division T cells (Arsenio et al., 2015). To determine the contribution of asymmetric inheritance of LFA-1 on the behavioral and differentiation phenotypes observed in LFA-1^{high} and LFA-1^{low} $CD8^+$ T cells, we sought to identify cytoplasmic molecules

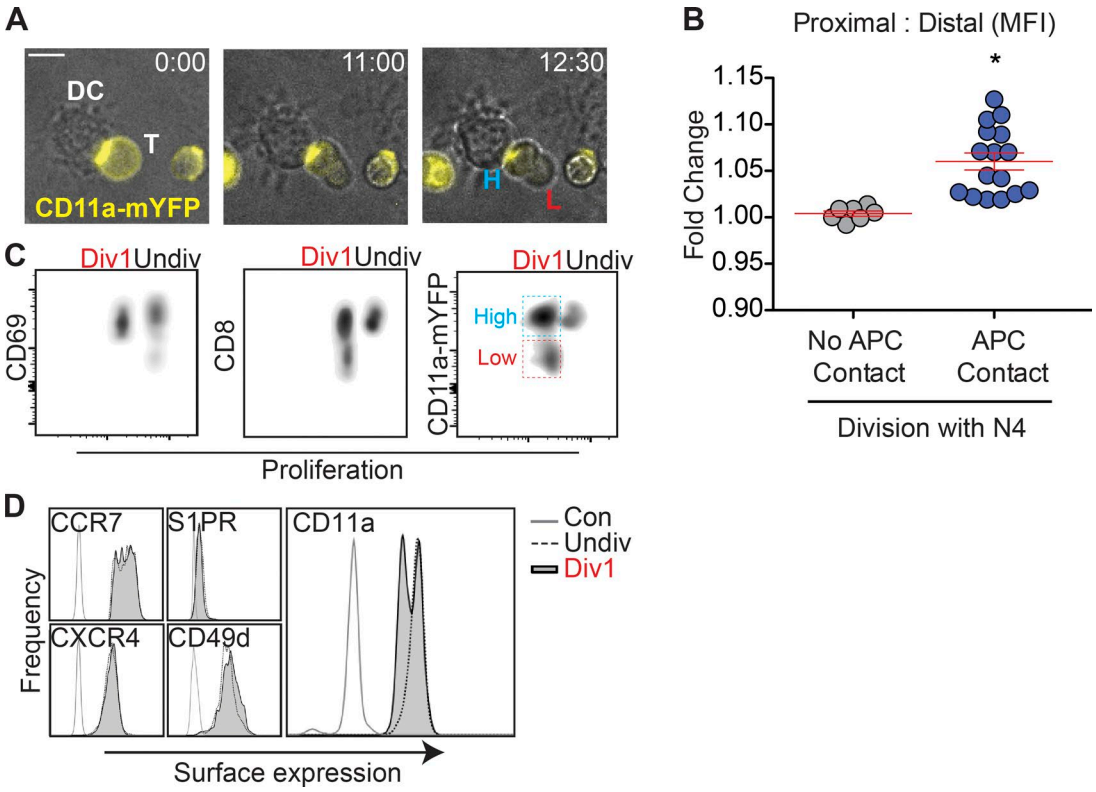

Figure 3. **Intracellular LFA-1 redistribution leads to unequal partitioning during division.** (A) Representative image of real-time cell division on ICAM-1–coated plates 30 h after co-culture of naive CD11a-mYFP/OT-I $CD8^+$ T cells (yellow) with N4-pulsed BMDCs. H, LFA-1^{high}; L, LFA-1^{low}. Bar, 5 µm. (B) Quantification of relative LFA-1 expression levels (mYFP intensity) of daughter T cells with and without APC contact during division. Data were analyzed based on real time imaging under N4-conditions. Each circle represents the ratio of total YFP intensity in each daughter cell by proximity to APC (proximity vs. distal). For divisions occurring outside of APC contact (no APC contact), proximity was assigned arbitrarily and both proximal and distal cells from the same parent cell showed similar YFP intensity (fold change = 1). Circles represent individual cells from five independent experiments with mean shown as a red line. Data represent mean ± SEM; $n = 5$. *, $P < 0.0003$. (C) Naive CD11a-mYFP/OT-I $CD8^+$ T cells ($1–3 \times 10^6$) were labeled with Cell Proliferation Dye eFluor670 and i.v. transferred 24 h before infection with influenza virus x31-OVA. 56 h after infection, transferred cells were sorted and identified as the first division (Div1) and undivided (Undiv) cells based on proliferation dye dilution. Cell surface CD8 and CD11a-mYFP showed asymmetric expression on the first-divide cells (Div 1), but not the cell activation marker (CD69). Results are representative of 10 independent experiments (one mouse per experiment). (D) Flow cytometry analysis of cell surface receptors of the first division (Div1) and undivided (Undiv) $CD8^+$ T cells generated from OT-I mice 56 h after infection with influenza virus x31-OVA (as described in C). Transferred cells were sorted on proliferation dye expression and stained for cell surface receptors, Con, isotype control. Results are representative of three independent experiments (one mouse per experiment).

required for the redistribution of intracellular LFA-1 to the cell surface. Based on the molecular model of YFP expression in our CD11a-mYFP mice (Fig. 5 A), we predicted that an anti-YFP antibody would selectively isolate LFA-1–containing endosomes from $CD8^+$ T cells. To confirm this hypothesis, we first isolated the total endosomes from homogenized CD11a-mYFP $CD8^+$ T cells using flotation ultracentrifugation (Fig. 5 B, left) and selectively immunoprecipitated CD11a-$mYFP^+$ endosomes using beads coated with a monoclonal GFP (E36) antibody that cross-reacts with YFP. Western blot analysis with a polyclonal YFP antibody was used to distinguish CD11a-$mYFP^+$ and CD11a-$mYFP^-$ endosome fractions (Fig. 5 B, right). To confirm that the majority of the intracellular CD11a is paired with CD18 and thus forms intact LFA-1 heterodimers in the CD11a-$mYFP^+$ endosomal compartments, YFP^+ endosomes from naive CD11a-mYFP/$CD8^+$ T cells were analyzed on a native-PAGE together with total cell lysate. Immunoblotting with anti-GFP (to detect CD11a-mYFP) or anti-CD18 antibody revealed a single band presumably corresponding to an intact heterodimeric LFA-1 (CD11a-mYFP/CD18) with both antibodies and no evidence of unpaired single subunit of CD11a or CD18 was detected (Fig. 5 C). We then compared these immunoblots with those of denatured samples and observed a band at ∼180 kD with anti-GFP corresponding to the CD11a-mYFP single chain and a band at ∼95 kD with anti-CD18 corresponding to single-chain CD18 of LFA-1 (Fig. 5 C). Therefore, this approach allowed us to fractionate a highly purified LFA-1^+ endosome population free of cytosolic and cell membrane contaminants.

Using this highly pure endosome fraction, we first confirmed that LFA-1^+ endosomes are not associated with $CD3\zeta^+$ endosomes required for TCR signals (Fig. 5 B, right). To further investigate a potential cell-recycling pathway associated with LFA-1^+ endosomes in naive T cells, we screened purified LFA-1^+ endosomes isolated from naive CD11a-mYFP $CD8^+$ cells for the presence of Rab proteins linked to exocytic and endocytic vesicle trafficking pathways. Among the Rab proteins we evaluated, Rab27 exclusively localized to LFA-1^+ endosomes and was not observed in LFA-1^- endosomes (Fig. 5 D).

In effector $CD8^+$ T cells, Rab27 is responsible for docking of cytolytic granules to the membrane of the killing synapse (Haddad et al., 2001; Stinchcombe et al., 2001). However, the role of Rab27 in naive $CD8^+$ T cells remains undefined. Membrane and intracellular LFA-1 levels, migration, conjugate formation, initial TCR activation, and lymph node homing of naive

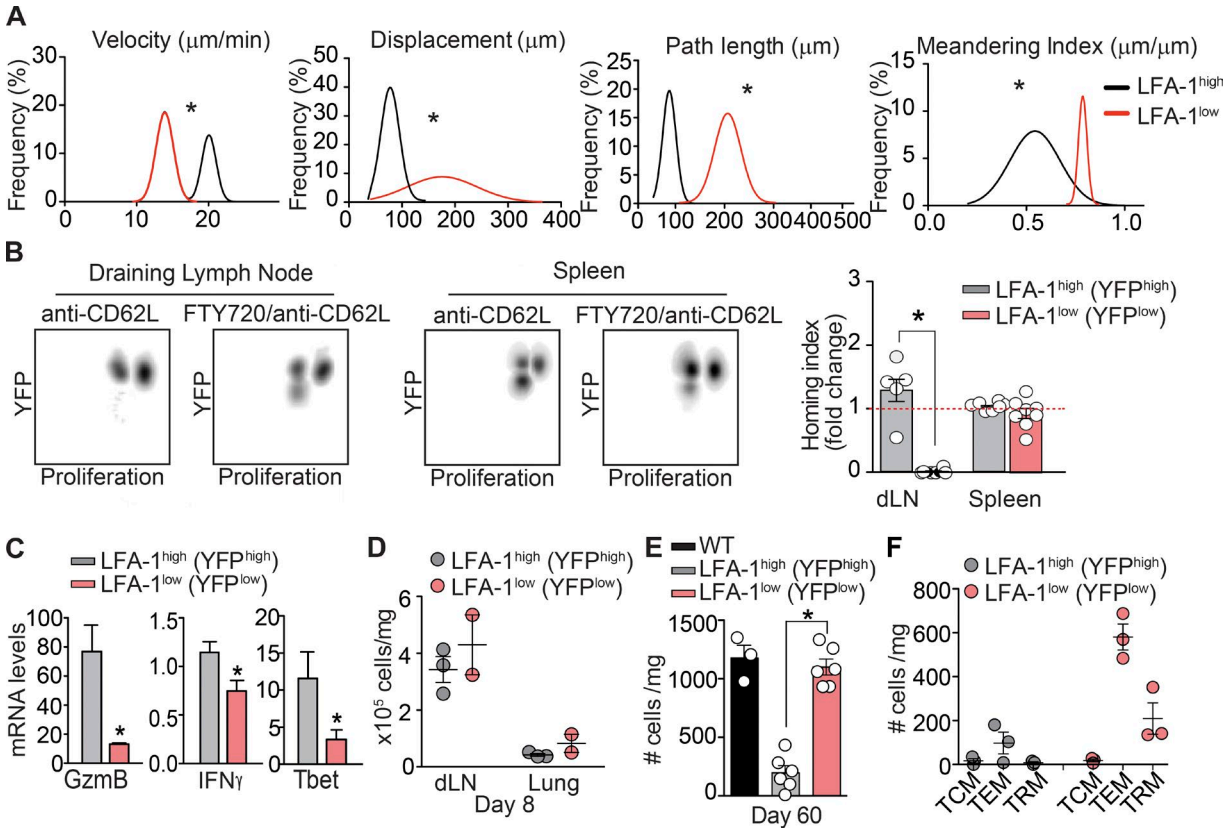

Figure 4. **Unequal LFA-1 expression leads to disparate migration and differentiation of first-division CD8⁺ T cells.** (A) Frequency distribution of migration indices measured from sorted first-division LFA-1^{high} (YFP^{high}) versus LFA-1^{low} (YFP^{low}) CD8⁺ T cells migrating on ICAM-1+CCL21–coated plates were significantly different. Data collected from four independent experiments (one mouse per experiment; 44–72 cells per mouse) were fit to nonlinear regression, and multimodality was assessed with the Kolmogorov–Smirnov test. Asterisk indicates significance between LFA-1^{high} versus LFA-1^{low} (*, P < 0.01). (B) Flow cytometry analysis and homing index of first-division LFA-1^{high} versus LFA-1^{low} CD8⁺ T cells generated in vivo in x31-OVA–infected mice treated with 100 µg anti-CD62L i.v. ± 1 µg/g FTY720 i.p. 44 hpi. Lymph node and spleen were harvested at 56 hpi, and single-cell suspension was recorded on a flow cytometer (left). The homing index (right) of Div1 YFP^{high} or Div1 YFP^{low} cells was calculated as the ratio between anti-CD62L–treated mice and (anti-CD62L + FTY720)–treated mice. Circles represent individual mice from three independent experiments (one or two mice per experiment) with mean shown as a line. Data represent mean ± SEM. *, P < 0.0001. (C) mRNA levels of indicated genes from sorted first-division LFA-1^{high} versus LFA-1^{low} CD8⁺ T cells from x31-OVA–infected mice 56 hpi. Data represent mean ± SEM; *n* = 3 mice per group. *, P < 0.05. (D and E) First-division LFA-1^{high} and LFA-1^{low} CD8⁺ T cells were harvested at 56 hpi from influenza-infected mice and sorted based on YFP expression. Equal numbers (2 × 10^3) of sorted first-division LFA-1^{high} versus LFA-1^{low} CD8⁺ T cells were injected into WT recipients, and mice were then inoculated with X31-OVA. The number of CD11a-mYFP⁺ CD8⁺ T cells found in the draining lymph node and lung 8 dpi (D; *n* = 3 mice per group) or 60 dpi (E) is shown. Data represent mean ± SEM; *n* = 3–6 mice per group. *, P < 0.001) as measured by flow cytometry. (F) Number of tissue-resident memory (TRM; CD103⁺ [integrin α_E], CD62L^{low} [L-selectin], CD44^{high}), central memory (TCM; CD62L⁺, CD44^{high}), and effector memory (TEM; CD62L^{neg}, CD44^{high}) CD11a-mYFP⁺ CD8⁺ T cells found in the lung 60 dpi. Data represent mean ± SEM; *n* = 3 mice/group. *, P < 0.001.

CD8⁺ T cells from Rab27 KO mice were comparable to naive CD8⁺ T cells from WT mice (Fig. 6 A and Fig. S5, A–I). However, the redistribution of intracellular LFA-1 to the cell surface (Fig. 6 C) and the contact site with APCs (Fig. 6 B) was completely abolished in CD11a-mYFP/OT-I/Rab27 KO T cells. Importantly, CD11a-mYFP/OT-I/Rab27 KO CD8⁺ T cells failed to induce asymmetric inheritance of both LFA-1 and CD8 after the first division and their retention time in the draining lymph node was comparable to LFA-1^{high} CD8⁺ T cells (Fig. 6 D). Additionally, the first-division CD8⁺ T cells from CD11a-mYFP/OT-I/Rab27 KO mice (KO Div 1) failed to exhibit similar bimodal patterns of cell migration as WT divided cells (WT Div 1; Fig. 6 E). The frequency of APC conjugation of KO Div 1 versus WT Div 1 CD8⁺ T cells was measured. Among the cells imaged, 45% of WT Div 1 T cells spent more than 70% of imaging time forming stable contacts with OVA-loaded APCs, whereas the rest of the cells only made transient contacts. In contrast, the majority of KO Div 1 T cells (65% of total) never or only transiently (less than 30% of imaging time) contacted APCs. Therefore, we concluded that Rab27-mediated LFA-1 redistribution is a key regulator of the unequal partitioning of LFA-1 during the T cell division, which is critical for the distinct patterns of migration and APC conjugation during T cell differentiation (Fig. 4, A and B).

To corroborate our hypothesis that the differential expression of LFA-1 is the key functional determinant that dictates the distinct migration patterns of first-division LFA-1^{high} proximal and LFA-1^{low} distal daughter T cells, we evaluated OT-I/CD11a heterozygous KO mice (LFA-1 Het). Reduction of LFA-1 surface expression by 49–57% in LFA-1 Het T cells (Fig. 7 A) did not alter early T cell activation, such as APC conjugation, CD69 and CD25 expression, and redistribution of intracellular LFA-1 expression, in naive LFA-1 Het compared with WT CD8⁺ T cells (not depicted). However, reduced LFA-1 expression levels abolished the polarized localization of intracellular LFA-1 to the contact site between T cells and APCs and subsequent

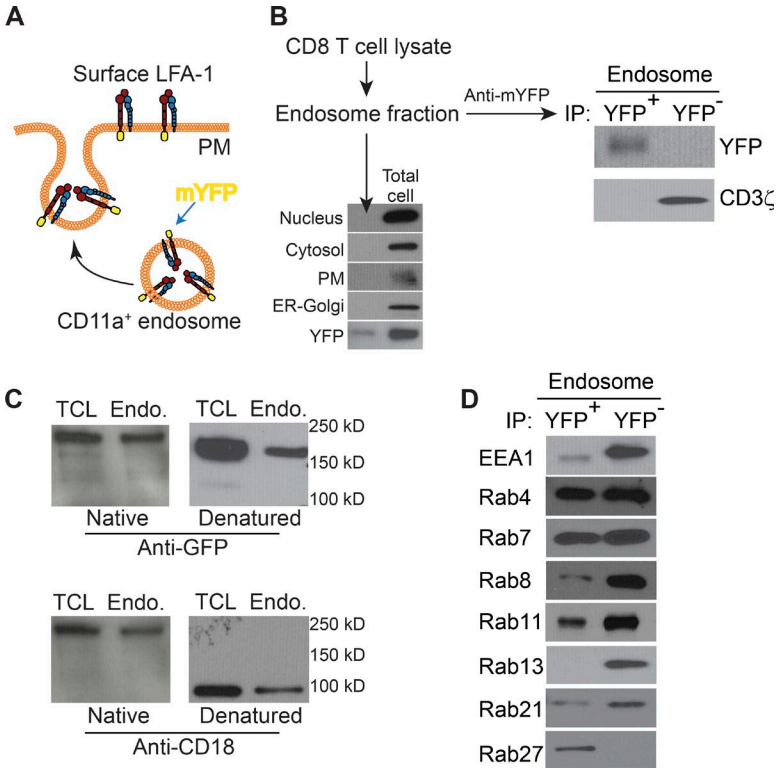

Figure 5. **Intracellular LFA-1 contained in Rab27 endosomes.** (A) Schematic depicting the mYFP tag on the exterior of LFA-1+ endosomes. (B) Purity of endosomal fraction isolated from naive CD11a-mYFP/CD8+ T cell homogenate was confirmed by the absence of lamin B (nucleus marker), HSP90 (cytosol maker), NaKATPase (plasma membrane [PM] marker), and SERCA1/2/3 (ER–Golgi marker) signals and the presence of CD11a-mYFP signal in Western blot analysis (left). LFA-1+ endosome and LFA-1− endosome were further separated by immunoprecipitation (IP) with a monoclonal GFP/YFP (E36) antibody and tested for the presence of CD3ζ (right). Results are representative of three independent experiments. (C) Total cell lysate (TCL) and LFA-1+ endosome lysate (Endo) were isolated under native conditions (native) and tested for the presence of intact LFA-1 heterodimer, and compared with endosomes and TCL isolated under denaturing conditions (denatured) for the presence of CD11a-mYFP (180 kD) and CD18 (~95 kD). Results are representative of three independent experiments. (D) LFA-1+ and LFA-1− endosomes were tested for indicated Rab protein expression. Results are representative of six independent experiments.

differential expression of LFA-1 in the first-division CD8+ T cells (Fig. 7, B and C). Importantly, the lack of asymmetric expression of LFA-1 in first-division T cells completely abolished the distinct patterns of T cell migration and APC interactions observed in WT first-division T cells (Fig. 7 D). Although our studies with LFA-1 Het T cells do not define the role of LFA-1 under normal physiology, these data suggest that asymmetric expression levels of LFA-1 in the first-divided CD8+ T cells are essential for the distinct motility pattern, which may lead to the differential fates of daughter CD8+ T cells. To corroborate our hypothesis that differential expression (high vs. low) of LFA-1 has an immunological consequence, we performed T cell memory experiments using Rab27 KO and LFA-1 Het mice. Because asymmetric cell division does not occur in these cells and there are no YFP high/low cells in the first division, we sorted total division 1 cells and transferred them into a naive WT recipient. We then infected the recipient mice with influenza virus and assessed the ability of Rab27 KO and LFA-1 Het cells to form T cell memory. Unlike WT T cells, Rab27 KO and LFA-1 Het T cells were unable to form the central memory, effector memory, and tissue-resident memory compartments 60 dpi (Fig. 7 E), suggesting that cell surface LFA-1 expression plays a key role in immunological memory formation.

Discussion

In this study, we generated CD11a-mYFP KI mice that allowed us to identify novel intracellular LFA-1 endosomes, which actively redistribute to the cell surface upon antigen stimulation. Redistribution and sequestration of LFA-1 to the immunological synapse during early T cell activation was required for unequal partitioning of LFA-1 into first-division daughter cells. Subsequent isolation of daughter T cells with unequal LFA-1 expression further revealed different functional phenotypes with distinct patterns of migration, APC conjugation, lymph node retention, and T cell effector programs. Interestingly, our in vivo egress assay demonstrated LFA-1^{low} cells egress from the lymph node faster than LFA-1^{high} cells, suggesting these cells may home to other tissues. It is possible that LFA-1^{low} T cells migrate to other lymphoid organs to create additional inflammatory niches or that they reenter the same lymph node at a later time point after the tissue established a favorable microenvironment that facilitates altered differentiation. Alternatively, a highly migratory phenotype of LFA-1^{low} T cells may enable them to rapidly egress from the lymph node and home in to target peripheral tissues. These events might promote long-term developmental plasticity to enable both self-renewal and terminal differentiation at the target tissue sites. Therefore, we conclude that dynamic redistribution of intracellular LFA-1 during early antigen stimulation controls T cell differentiation and effector functions of daughter cells.

Recent studies have shown that important mediators of LFA-1 functions, including Rap1, Rap2, RapL, and Mst1, are contained in Rab5, Rab11, Rab13, and EEA1 vesicles (Fabbri et al., 2005; Stanley et al., 2012; Svensson et al., 2012; Nishikimi et al., 2014) and that LFA-1 is endocytosed and recycles through a cholesterol- and Rab11-dependent manner through a YXXΦ motif in the cytoplasmic region of the β_2 subunit (Fabbri et al., 2005). However, the presence of LFA-1 in these endosomal cargo and functions of the intracellular LFA-1 in naive T cell activation remains unknown. In addition to detection of endogenous LFA-1 redistribution in live T cells, our CD11a-mYFP KI mice allowed us to isolated highly pure LFA-1+ endosomes from naive T cells using anti-YFP immunoprecipitation. Our Western blot analysis with a polyclonal YFP antibody to isolate CD11a+ endosome fractions revealed that Rab27 localized exclusively to LFA-1+ endosomes and was not observed in

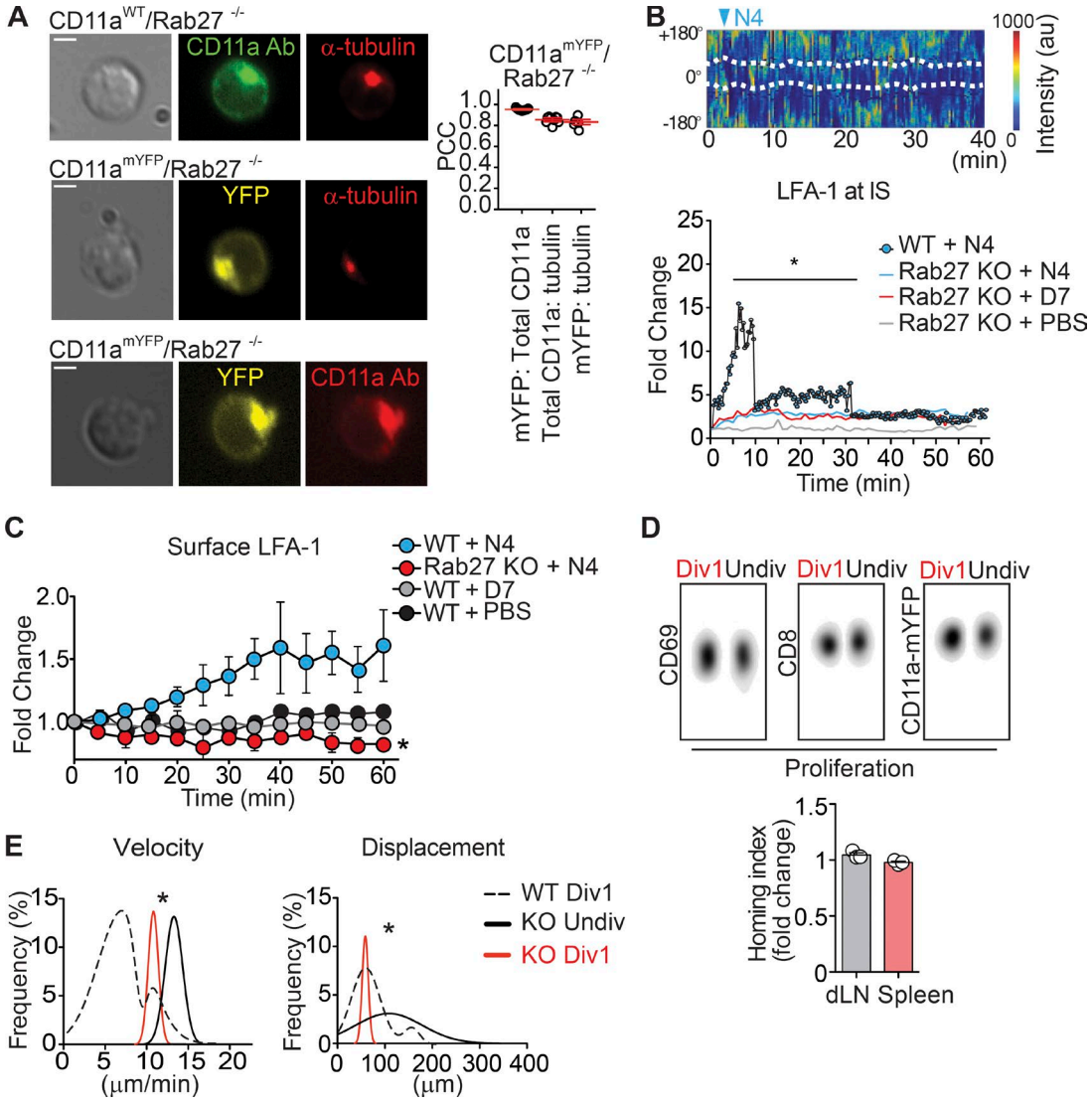

Figure 6. **Rab27-mediated intracellular LFA-1 redistribution mediates differential behavior of first-division cells.** (A) Representative images showing both surface and intracellular staining (permeabilized with 0.05% saponin) of LFA-1 (green: anti-CD11a, clone M17/4) and α-tubulin (red: clone 11H10). Bars, 2 µm. Pearson's correlation coefficients from naive CD11a-mYFP/OT-I/Rab27 KO CD8+ T cells (right). Each dot represents mean PCC from one mouse (30–45 cells/mouse). (B) Representative mYFP fluorescence intensity from the CD11a-mYFP/OT-I/Rab27 KO CD8+ T cell surface (top). YFP fluorescence intensity is shown in a pseudocolor scale (from low [black] to high [red]). +/− 180°, rear of cell; 0°, leading edge; white lines depict the T cell–APC interface; arrowheads indicate the beginning of the T cell–APC contact. Quantification of relative fluorescence intensity of mYFP from CD11a-mYFP/OTI (WT) versus CD11a-mYFP/Rab27KO/OT-I (Rab27 KO) cells at the contact site (bottom). Data are expressed as mean of total 35–55 cells. *, $P < 0.001$. (C) Flow cytometry measuring LFA-1 surface levels (anti–LFA-1 antibody) on T cells from OT-I (WT) or OT-I/Rab27 KO after indicated times of T and N4-, D7-, or PBS-loaded APC contacts. Data are expressed as mean ± SEM of three separate experiments (8–10 mice/group). *, $P < 0.0001$. (D, top) Representative flow cytometry of CD11a-mYFP/OT-I/Rab27 KO CD8+ T cell division in x31-OVA infected mice 56 hpi ($n = 9$). (D, bottom) The homing index of Div1 Rab27 KO was calculated as the ratio between CD62L-treated mice and (CD62L + FTY720)–treated mice. Circles represent individual mice from three independent experiments (one mouse per experiment) with mean shown as a line. (E) Frequency distribution of migration velocity and displacement measured from WT-OTI (WT Div1) and OT-I/Rab27 KO (KO Div1) first-division or undivided OT-I/Rab27 KO (KO Undiv) CD8+ T cells migrating on ICAM-1+CCL21–coated plates. Data collected from three independent experiments (one mouse per experiment; 40–65 cells/mouse) were fit to nonlinear regression, and multimodality was assessed with the Kolmogorov–Smirnov test. Asterisk indicates significance between WT Div1 and KO Div1 (*, $P < 0.01$).

LFA-1− endosomes (Fig. 5 D). The results from in vitro and in vivo experiments with Rab27 KO CD8+ T cells (Fig. 6) strongly support our conclusion that Rab27 is a key regulator for trafficking of intracellular LFA-1 to the cell surface, an essential step for asymmetric segregation of LFA-1 into first-division daughter T cells and subsequent distinct patterns of migration and APC interactions during T cell activation.

Surprisingly, we observed an extreme enrichment of LFA-1 at the point of contact between T cells and APCs during the early phase (<10 min) of immunological synapse formation, followed by prolonged accumulation of LFA-1 at the contact zone for 60 min (an ∼5-fold increase until 30 min and an ∼2.5-fold increase between 30 min to 60 min; Fig. S3 C). TCR activation during the synapse formation triggers a cascade of signaling events, which may differentially regulate LFA-1 adhesiveness and distribution. In addition to the intracellular signals that directly regulate LFA-1 functions, centripetal flow of T cell actin cytoskeleton recruits LFA-1 to the synapse and induces mechanical maturations of distinct affinity status (Comrie et al., 2015). Interestingly, analysis of T cell–APC interaction

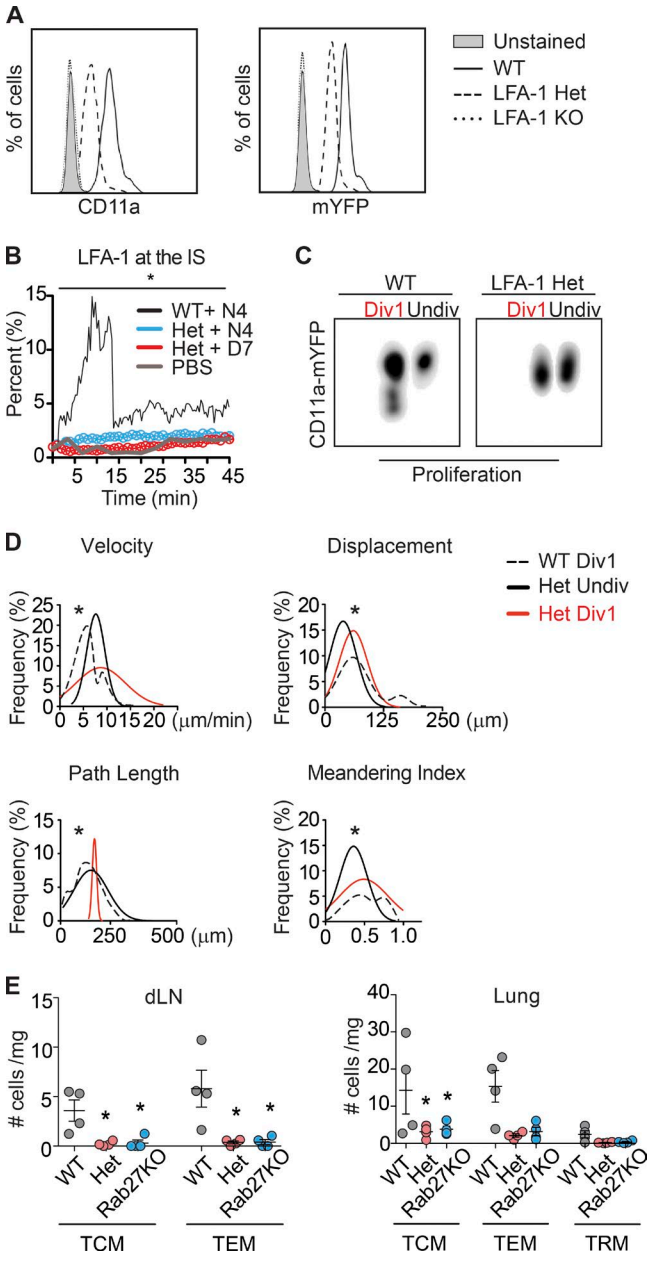

Figure 7. **CD11a heterozygous knockout T cells fail to induce asymmetric LFA-1 expression and disparate migration patterns in first-division CD8⁺ T cells.** (A) Representative flow cytometry of surface (CD11a Ab) and total (mYFP) LFA-1 expression levels from CD11a-mYFP/OT-I Het and WT OT-I naive CD8⁺ T cells; $n = 3$ mice. (B) Quantification of relative fluorescence intensity of mYFP from CD11a-mYFP/OTI (WT) versus CD11a-mYFP/OT-I Het CD8⁺ T cells at the contact site with Ag-bearing APCs (N4 or D7). Data are expressed as mean of total 25–40 cells. (C) Representative flow cytometry analysis of asymmetric expression of CD11a-mYFP in WT (CD11a-mYFP/OT-I) versus LFA-1 Het (CD11a$^{+/-}$-mYFP/OT-I) CD8⁺ T cell division from x31-OVA–infected mice 56 hpi; $n = 6$ mice. (D) Frequency distribution of migration indices measured from CD11a-mYFP (WT Div1) and CD11a-mYFP$^{+/-}$ (Het Div1) first-division or CD11a-mYFP$^{+/-}$ (Het Undiv) undivided CD8⁺ T cells. Data collected from three independent experiments (one mouse per experiment; 45–60 cells/mouse) were fit to nonlinear regression and multimodality was assessed with the Kolmogorov–Smirnov test. Asterisk indicates significance between WT Div1 and Het Div1 (*, $P < 0.01$). (E) Number of tissue-resident memory (TRM; CD103⁺ [integrin α_E], CD62L^{low} [L-selectin], CD44^{high}), central memory (TCM; CD62L⁺, CD44^{high}), and effector memory (TEM; CD62L^{neg}, CD44^{high}) CD11a-mYFP⁺ CD8⁺ T cells found in the draining lymph node and lung 60 dpi (CD11a$^{+/-}$-mYFP/OT-I T cells: Het, CD11a-mYFP/OT-I/Rab27 KO T cells: Rab27KO). Data represent mean ± SEM; $n = 4$ mice/group. *, $P < 0.05$.

with atomic force microscopy revealed that forces between the cell–cell contacts in the presence of antigen increased from 1 to 2 nN at early time points to a maximum of ≈14 nN after 30 min and decreased to the basal level after 60 min (Hosseini et al., 2009). Therefore, we speculate that the dramatic enrichment of LFA-1 at the initial T cell–APC contact site may be mediated by "quick" lateral redistribution of low or intermediate affinity LFA-1 before it is replaced by a smaller number of high affinity LFA-1, likely derived from the intracellular pool that is tightly associated with actin cytoskeleton and distinct signaling molecules, which eventually leads to asymmetric partitioning into two daughter cells after division. It is also important to note that CD8⁺ T cells engage in several APC contacts during activation and before their first division (Mempel et al., 2004; Eickhoff et al., 2015). Thus, several T cell–APC immunological synapses have to form during this time, and the immunological synapse present while the T cell divides is not necessarily the same immunological synapse that induces LFA-1 redistribution in our imaging.

Our study provides insight into how the differential migration patterns mediated by disparate LFA-1 expression control daughter T cell migration and their fates. Important functions of LFA-1 in T cell adhesion on the high endothelial venules and subsequent transendothelial migration to enter the lymph node are well characterized (Shulman et al., 2009; Hogg et al., 2011). Unlike T cell entry, it was proposed that integrins are not absolutely required for T cell motility in the lymph node (Woolf et al., 2007). A recent study, however, demonstrated that LFA-1 blockade abolished high velocity migration of naive T cells in the lymph node (Katakai et al., 2013), suggesting that LFA-1–mediated migration is important for the speed and pattern of T cell migration in the lymph node. Similarly, perturbation of important intracellular molecules that regulate LFA-1 functions, such as Rap1 and RhoH, showed significant changes in T cell migration in the lymph node (Kinashi and Katagiri, 2004; Baker et al., 2012). Moreover, T cells deficient in LFA-1 egress the lymph node at a faster rate than WT T cells (Reichardt et al., 2013), suggesting LFA-1 plays an important role in T cell retention. It is also important to note that although LFA-1–independent migration occurs under depleting conditions, the outcome of the immune response may be altered. Indeed, both blockade and deficiency of LFA-1 demonstrated that LFA-1 is crucial for prolonged T cell–APC interactions and efficient T cell activation, as T cells are unable to proliferate, generate cytokines, and differentiate without intact LFA-1 functions (Salomon and Bluestone, 1998; Kandula and Abraham, 2004; Varga et al., 2010). LFA-1–deficient T cells are also incapable of participating in T–T interactions during T cell activation, which is an LFA-1–mediated event important for T cell survival and proliferation signals (Doh and Krummel, 2010; Gérard et al., 2013).

It was proposed that the asymmetric inheritance of fate determinants establishes effector and memory CD8⁺ T cell development (Chang et al., 2007, 2014; Arsenio et al., 2014). Prolonged interactions with APCs and additional signals from the immune niche provide CD8⁺ T cells the opportunity to divide while maintaining the intracellular asymmetry that arose from TCR signaling. Additionally, activation of several important T cell transcription factors, such as T-bet, Eomes, and Runx, is regulated by T cell–APC dwell time, signal accumulation, and cytokine exposure (Yeo and Fearon, 2011; Xin et al., 2016). The unifying theme between these events is integrin-mediated adhesion during migration and cell–cell interactions, for which

$CD8^+$ T cells primarily use LFA-1 (Van Seventer et al., 1990; Berlin-Rufenach et al., 1999; Wang et al., 2009; Contento et al., 2010; Varga et al., 2010; King et al., 2012). Although previous studies highlighted the importance of LFA-1 interactions with its ligand ICAM-1 in $CD8^+$ T cell memory development (Parameswaran et al., 2005; Ghosh et al., 2006; Scholer et al., 2008; Bose et al., 2013; Cox et al., 2013; Zumwalde et al., 2013), a direct link between LFA-1 and memory formation has yet to be identified. Our study provides insight into how the differential migration patterns mediated by asymmetric expression of LFA-1 control the fate decisions of daughter T cells.

The selectivity of naive $CD8^+$ T cells to redistribute intracellular LFA-1 in recognition of strong, but not weak, antigenic stimulation suggests that cell surface LFA-1 expression may serve as an evolutionarily conserved mechanism in T cells. Such selectivity may ensure that the immune system uses the Rab27-mediated mechanism during appropriate immune activation against highly pathogenic infections. It would be interesting to investigate whether diversity in T cell memory is due, at least in part, to distinct LFA-1 redistribution patterns and thus changes in the occurrence of unequal LFA-1 partitioning during cell division by pathogens with different antigenicity. However, further studies to investigate direct roles of Rab27 in T cell memory formation in our system are infeasible, as examining memory T cell development in Rab27 KO is limited by the inability of these mice to clear primary infection. Both LFA-1 and Rab27 play critical roles in cytotoxic T cell functions, and although the host immune system can clear viral infection, the transferred KO T cells would subsequently differentiate in altered conditions. Nevertheless, further elucidating the contribution of LFA-1 in memory generation at later stages of T cell activation may be critical for future therapeutic developments.

Materials and methods

Antibodies and reagents

CCR7-PE (4B12), CXCR4-PE (2B11), CD11a-eFluor450 (M17/4), CD25-APC (PC61.5), purified CD62L (MEL-14), CD4-PE (GK1.5), MHCI-APC (H2Kb; AF6-88.5.5.3), and OneComp eBeads were purchased from eBioscience. CD69-PE/Cy7 (H1.2F3), Va2-APC (B20.1), VB5.1, 5.2-PE (MR9-4), CD8-PerCP (53–6.7), and CD19-PE/Cy7 (1D3) were purchased from BD Biosciences. CD49d (R1-2), LFA1-PE (H155-78), CD11a-AF647 (M17/4), CD11a-AF488 (M17/4), CD69-APC (H1.2F3), CD69-BV605 (H1.2F3), CXCR5-BV421 (L138D7), CXCR3-BV421 (CXCR3-173), CD107a-AF647 (1D4B), and Gr1-AF488 (RB6-8C5) were purchased from BioLegend. S1PR-PE (713412) was purchased from R&D. β-Actin (AC-15), pCD3ζ ($pTyr^{142}$), and OptiPrep Density Gradient Medium were purchased from Sigma. HSP90 (2D11B9) was purchased from Enzo. Na-K-ATPase was purchased from CST. Lamin B1 (EPR8985B) was purchased from CST from Abcam. SERCA1/2/3 (H-300), IP3R1 (CT1), and IP3R2 (NT2) were provided by D. Yule (University of Rochester, Rochester, NY). Exo1 and Dynasore were purchased from Tocris. For intracellular staining, cells were fixed with 4% formaldehyde then treated with 0.05% saponin (Sigma) before staining. To obtain cytosolic and plasma membrane fractions, cells were processed with a Subcellular Protein Fractionation kit (Thermo). For RNA extraction, cells were homogenized with QIAshredder (Qiagen) and processed with PureLink RNA Mini kit (Ambion). cDNA was generated with iScript DNA Synthesis kit (Bio-Rad) and measured on ABI7300 Real Time PCR System (Applied Biosystems) in TaqMan Gene Expression Master Mix (Applied Biosystems) with *Gzmb*, *Tbx21*, and *ifng* FAM-probes (Thermo). To assess peptide stability on MHC class I, RMA-S cells (provided by J. Frelinger, University of Rochester, Rochester, NY) were pulsed with various concentrations of peptide for 1 h, washed extensively, and incubated for 3 h at 37°C. MHC class I (H2Kb) antibody (AF6-88.5.5.3; eBioscience) was used to detect surface levels by flow cytometry.

Mice

C57BL/6 and OT-I TCR transgenic (C57BL/6-Tg(TcraTcrb)1100Mjb/J) mice were purchased from the Jackson Laboratory. CD11a-mYFP mice were generated at the Gene Targeting and Transgenic Core facility at the University of Rochester using similar gene targeting techniques previously used in our laboratory to generate the CD18-mCFP mice and the K562 FRET cell line (Kim et al., 2003; Hyun et al., 2012). Of note, the mYFP gene was fused to the last exon (exon 31) of the CD11a gene with a 5-aa linker (GPVAT; Kim et al., 2003). These mice were backcrossed with OT-I mice for at least 12 generations. C3H/HeSn-*Rab27a*^{ash}/J (ashen) were purchased from Jackson Laboratory and bred with CD11a-mYFP/OT-I to generate CD11a-mYFP/OT-I/Rab27 KO. Experiments with these mice used their littermates as controls and recipients. Genotyping for each strain was performed according to the corresponding reference. All mice were maintained in a pathogen-free environment of the University of Rochester animal facility, and the animal experiments were approved by the University Committee on Animal Resources at the University of Rochester (Rochester, NY).

Leukocyte and BMDC preparation

$CD8^+$ T cells were prepared from negative selection via DynaBeads (Invitrogen) or $CD8a^+$ T Cell Isolation kit (Miltenyi) with 93–99% purity. Cells were stained with CFSE (Thermo) or Cell Proliferation Dye eFluor670 (eBioscience) before injection and culture. In MTOC studies, cells were stained with ER Tracker (Molecular Probes) for live tracking or a-tubulin-AF647 (11H10; CST) for fixed images. For calcium studies, cells were stained with Calcium Crimson, AM (Thermo) as per the manufacturer's instructions. Where indicated, $CD8^+$ T cells were in vitro activated with donor irradiated splenocytes with 10 µm OVA-peptide (pOVA) + IL-2 in complete media for 5 d. For killing assays, activated $CD8^+$ T cells were co-cultured for 4 h with 10 µm Ag-pulsed EL-4 cells (ATCC) labeled with PKH26 (Sigma). CD107a-AF647 (1D4B; BioLegend) and Annexin V-APC (eBioscience) were used to detect degranulation and killing, respectively. To generate BMDCs, bone marrow was harvested and plated in media containing 5% FBS + 20 ng/ml granulocyte macrophage colony-stimulating factor (BioLegend). Cells were used between day 8 and 14 of culture and confirmed by MHC II (M5/114; BioLegend) and CD11c (N418; BioLegend) expression. BMDCs were activated with 1 µg/ml lipopolysaccharide (Sigma) 12 h before use, and activation was confirmed by CD80 (16-10A1; BioLegend) and CD86 (GL-1; BioLegend) expression. BMDCs were pulsed with 10 µm pOVA for 2 h, washed extensively, and allowed to adhere on delta-T dishes for 1 h before imaging.

Cell transfers and infections

Naive $CD8^+$ T cells ($1–3 \times 10^6$) were i.v. transferred 24 h before influenza infection or footpad injections. For influenza studies, 8- to 12-wk-old mice were anesthetized using Avertin (2,2,2-tribromoethanol) and intranasally inoculated with 30 µl influenza A virus suspension (HKx31-OVA, $3 \times 10^{3.25}$ EID50). Draining lymph node and spleen were harvested at 56 h post invasion (hpi), enriched for $CD8^+$ cells (Miltenyi), and sorted for described populations. Alternatively, the footpad of mice were injected with 25 µg pOVA (N4: SIINFEKL) plus

25 µg lipopolysaccharide (Sigma). Where noted, altered peptide ligands were used at the same concentration (D7: SIINFE**D**L; BioPeptide).

Competitive egress assay

For the competitive egress assay, equal numbers of T cells (10^6 each) were differentially labeled and i.v. injected to WT recipients. Lymph nodes were harvested at 24 h, and single-cell suspensions were analyzed by flow cytometry. The homing index was calculated as the ratio between the number of each differentially-labeled cell population present. For the first-division egress assay, 100 µg anti-CD62L (BD) and 1 µg/g FTY720 (Cayman Chemicals) were injected i.v. and i.p., respectively, 12 h before harvest. The homing index of Div1 YFP^{high} or Div1 YFP^{low} cells was calculated as the ratio between CD62L-treated mice and (CD62L + FTY720)–treated mice.

T cell memory

For memory assays, LFA-1^{high} and LFA-1^{low} cells were harvested at 56 hpi from influenza-infected mice and sorted based on YFP expression. 2,000 LFA-1^{high} or LFA-1^{low} cells were transferred into a naive WT recipient. Mice were then inoculated with X31-OVA. To distinguish cells in the vasculature versus tissue, mice were treated with CD8β-APC (BD) i.v. 3 min before harvest. Draining lymph node, spleen, and lung were harvested 8 or 60 dpi. Macerated lung tissue was digested with 5 mg/ml collagenase/dispase (Roche) for 1 h at 37°C. To distinguish memory phenotypes, single-cell suspensions were stained with CD44-BV421 (BioLegend), CD62L-PE/Cy7 (BD), CD103-BV711 (BD), and TCRβ-BV605 (BD).

In vitro imaging

Cell migration chambers (Millicell EZ slide eight-well glass; Millipore; or Delta T dish; Bioptech) were prepared by coating their glass bottom with 5 µg recombinant mouse ICAM-1 (Sino Biological) in PBS with or without indicated chemokines. For in vitro migration imaging, leukocytes were placed in L15 medium (Invitrogen) in the chamber at 37°C and video microscopy was conducted using a TE2000-U microscope (Nikon) coupled to a CoolSNAP HQ CCD camera with a 20× objective (CFI Plan Fluor ELWD DM; Nikon) and 0.45 numerical aperture. For conjugation studies, 10 µm peptide-pulsed BMDCs adhered to a Delta T dish coated with ICAM-1 and 2 µg CCL21 (R&D) for 1 h before imaging. For division studies, BMDCs and naive CD8 T cells were cultured on ICAM-1–coated Delta T dish in complete media with IL-2 in a stagetop incubator (Oko Labs) at 37°C with 5% CO_2. Images were acquired 30 h after co-culture using 40× (CFI Plan Fluor ELWD DM) or 60× (CFI Plan Apo VC; Nikon) magnification objective and numerical apertures of 0.6 and 1.4, respectively. All images were acquired in NIS Elements (Nikon). Migration analysis was performed in Volocity software (PerkinElmer). Real-time division fluorescent measurements were performed using NIS Elements. Division was scored as occurring while in contact with an APC or out of contact with an APC. For divisions occurring out of contact with APCs, proximal and distal cells were defined arbitrarily. Real-time conjugate fluorescent intensities were measured in MATLAB (MathWorks). In brief, cell perimeter and contact site were defined in DIC image and x, y coordinates were then used to detect fluorescent intensity in YFP images. Intensity was normalized as percent of maximum for each frame and registered for contact site. Quantification of relative LFA-1 expression levels (mYFP intensity) was measured using a 60× oil objective. YFP imaging filters were from Chroma (HQ500/20X, Q515LP, and HQ535/30M).

Cell conjugation assay

For flow cytometry–based conjugation assays, BMDCs were labeled with PKH26 (Sigma) and pulsed with 10 µM antigen for 2 h. T cells were labeled with Cell Proliferation Dye eFluor670 (eBioscience). T cells and BMDCs were mixed at a 1:1 ratio for the indicated times, and conjugate frequencies were determined from the percentage of T cell–APC conjugates to the total number of T cells. All conjugate assays were normalized to no antigen controls (PBS-pulsed BMDCs). For image-based conjugation studies, 10 µM peptide-pulsed BMDCs adhered to a Delta T dish coated with ICAM-1 and 2 µg CCL21 (R&D) for 1 h before imaging. T cells were added at a 1:1 ratio for the indicated times, and conjugate frequencies were determined from live imaging. All conjugation studies were normalized to no antigen controls (PBS-pulsed BMDCs).

Flow cytometry

For flow cytometry-based LFA-1 surface studies, naive CD8$^+$ T cells were co-cultured with antigen-pulsed BMDCs for the indicated times, fixed, and stained for LFA-1 surface levels. Experiments were normalized to no-antigen controls (PBS-pulsed BMDCs), and fold change was determined from time 0 (T cells only, no BMDCs). We used a BD LSR II flow cytometer with a solid-state Coherent Sapphire blue laser (20–100 mW at 488 nm), and the emission signal was detected by an associated photomultiplier tube.

Endosome isolation and Western blot analysis

Purified CD8$^+$ T cells were homogenized as previously described (Graham, 2002) in Diluent (50 mM Hepes-NaOH, 500 mM KOAc, and 5 mM MgOAc) and Halt protease and phosphatase inhibitor with a 27G needle 25 times and mixed with 50% solution (Diluent, 0.25 mM sucrose; Optiprep) for a 30% density. The gradient was loaded from bottom to top with the following densities: 2 ml of 30% homogenate, 8 ml of 25%, and 2 ml of 5%. Gradients were subjected to 250,000 *g* for 3 h at 4°C. Endosomes were collected from the 25–5% interface and processed for immunoprecipitation with anti-GFP (mouse monoclonal 3E6; Molecular Probes) covalently linked to CrossLink IP beads (Pierce). YFP$^-$ endosomes were diluted in PBS and subjected to 100,000 *g* for 10 h at 4°C. Both YFP$^+$ beads and YFP$^-$ pellet were resuspended in Laemmli sample buffer (Bio-Rad) and boiled. For Western blotting, the membrane was blocked with 5% nonfat milk or 5% BSA in PBS plus 0.1% Tween 20 for 30 min after proteins were transfer from PAGEr Gold Precast 4–20% Tris-Glycine gel (Lonza). Blots were incubated overnight at 4°C with 1:1,000 of anti-GFP (ab290; Abcam), CD3z (H146-968; Thermo) EEA1 (CST), Rab4 (BD), Rab7 (CST), Rab8 (CST), Rab11 (Abcam), Rab13 (Abcam), Rab21 (Santa Cruz), and Rab27a (Santa Cruz). The membrane was then incubated with 1:5,000 horseradish peroxidase–conjugated anti–rabbit or anti–mouse Fc-specific IgG antibody (Jackson ImmunoResearch) for 1 h at room temperature. Protein was detected using Super Signal chemiluminescent reagent (Thermo). Where described, native PAGE Bis-Tris Gels (nonreducing) were used (Thermo).

Statistical analysis

All statistical tests were done with GraphPad Prism and Jmp Software (SAS). For frequency distribution analyses, nonlinear regression was performed and multimodality was assessed with the Kolmogorov–Smirnov test. Analyses of multiple variances were analyzed with two-way ANOVA with a Bonferroni post-test. Other analyses used one-way ANOVA with a Bonferroni post-test, unpaired *t* test, and Mann–Whitney when appropriate.

Online supplemental material

Fig. S1 shows LFA-1 expression and function in CD11a-mYFP mice. Fig. S2 shows expression of intracellular LFA-1 in naive CD8$^+$ T cells from WT and CD11a-mYFP mice. Fig. S3 shows LFA-1 redistribution

to the T cell surface. Fig. S4 shows correlation of CD11a-mYFP high and low populations with CD8 expression. Fig. S5 shows that LFA-1 expression and functions are comparable in naive CD8+ T cells from WT and Rab27 KO mice. Video 1 shows localization of LFA-1 in naive CD8+ T cells. Video 2 shows localization of LFA-1 during naive CD8+ T cell migration. Video 3 shows intracellular LFA-1 redistribution to the contact site with Ag-bearing APCs. Video 4 shows that intracellular LFA-1 fails to redistribute to the contact site upon encountering APCs bearing altered peptide ligands with reduced TCR affinity. Video 5 shows that CD8+ T cell asymmetrically divides in real time.

Acknowledgments

We thank Eric Harrower, Jennifer Wong, and Urmila Sivagnanalingam for their technical assistance.

This project was supported by the National Institutes of Health (grants HL087088 and AI102851 to M. Kim and grant F31AI112257 to T. Capece).

The authors declare no competing financial interests.

Author contributions: T. Capece conducted most of the experiments and performed the statistical analysis of the data; B.L. Walling helped with virus infection, mouse injections, and in vitro imaging. S. Bae performed cytotoxic T cell killing assay. K.-D. Kim and K. Lim helped with western blot analysis. H.-L. Chung designed MATLAB algorithm. D.J. Topham assisted with experimental design. M. Kim conceived and directed the study. T. Capece and M. Kim wrote the manuscript with suggestions from all authors.

Submitted: 16 September 2016
Revised: 13 January 2017
Accepted: 11 July 2017

References

Arsenio, J., B. Kakaradov, P.J. Metz, S.H. Kim, G.W. Yeo, and J.T. Chang. 2014. Early specification of CD8+ T lymphocyte fates during adaptive immunity revealed by single-cell gene-expression analyses. *Nat. Immunol.* 15:365–372. http://dx.doi.org/10.1038/ni.2842

Arsenio, J., P.J. Metz, and J.T. Chang. 2015. Asymmetric Cell Division in T Lymphocyte Fate Diversification. *Trends Immunol.* 36:670–683. http://dx.doi.org/10.1016/j.it.2015.09.004

Baker, C.M., W.A. Comrie, Y.M. Hyun, H.L. Chung, C.A. Fedorchuk, K. Lim, C. Brakebusch, J.L. McGrath, R.E. Waugh, M. Meier-Schellersheim, and M. Kim. 2012. Opposing roles for RhoH GTPase during T-cell migration and activation. *Proc. Natl. Acad. Sci. USA.* 109:10474–10479. http://dx.doi.org/10.1073/pnas.1114214109

Berlin-Rufenach, C., F. Otto, M. Mathies, J. Westermann, M.J. Owen, A. Hamann, and N. Hogg. 1999. Lymphocyte migration in lymphocyte function-associated antigen (LFA)-1-deficient mice. *J. Exp. Med.* 189:1467–1478. http://dx.doi.org/10.1084/jem.189.9.1467

Bose, T.O., Q.M. Pham, E.R. Jellison, J. Mouries, C.M. Ballantyne, and L. Lefrançois. 2013. CD11a regulates effector CD8 T cell differentiation and central memory development in response to infection with Listeria monocytogenes. *Infect. Immun.* 81:1140–1151. http://dx.doi.org/10.1128/IAI.00749-12

Cairo, C.W., R. Mirchev, and D.E. Golan. 2006. Cytoskeletal regulation couples LFA-1 conformational changes to receptor lateral mobility and clustering. *Immunity.* 25:297–308. http://dx.doi.org/10.1016/j.immuni.2006.06.012

Chang, J.T., V.R. Palanivel, I. Kinjyo, F. Schambach, A.M. Intlekofer, A. Banerjee, S.A. Longworth, K.E. Vinup, P. Mrass, J. Oliaro, et al. 2007. Asymmetric T lymphocyte division in the initiation of adaptive immune responses. *Science.* 315:1687–1691. http://dx.doi.org/10.1126/science.1139393

Chang, J.T., E.J. Wherry, and A.W. Goldrath. 2014. Molecular regulation of effector and memory T cell differentiation. *Nat. Immunol.* 15:1104–1115. http://dx.doi.org/10.1038/ni.3031

Chen, L., and D.B. Flies. 2013. Molecular mechanisms of T cell co-stimulation and co-inhibition. *Nat. Rev. Immunol.* 13:227–242. http://dx.doi.org/10.1038/nri3405

Choudhuri, K., D. Wiseman, M.H. Brown, K. Gould, and P.A. van der Merwe. 2005. T-cell receptor triggering is critically dependent on the dimensions of its peptide-MHC ligand. *Nature.* 436:578–582. http://dx.doi.org/10.1038/nature03843

Ciocca, M.L., B.E. Barnett, J.K. Burkhardt, J.T. Chang, and S.L. Reiner. 2012. Cutting edge: Asymmetric memory T cell division in response to rechallenge. *J. Immunol.* 188:4145–4148. http://dx.doi.org/10.4049/jimmunol.1200176

Comrie, W.A., A. Babich, and J.K. Burkhardt. 2015. F-actin flow drives affinity maturation and spatial organization of LFA-1 at the immunological synapse. *J. Cell Biol.* 208:475–491. http://dx.doi.org/10.1083/jcb.201406121

Contento, R.L., S. Campello, A.E. Trovato, E. Magrini, F. Anselmi, and A. Viola. 2010. Adhesion shapes T cells for prompt and sustained T-cell receptor signalling. *EMBO J.* 29:4035–4047. http://dx.doi.org/10.1038/emboj.2010.258

Cox, M.A., S.R. Barnum, D.C. Bullard, and A.J. Zajac. 2013. ICAM-1-dependent tuning of memory CD8 T-cell responses following acute infection. *Proc. Natl. Acad. Sci. USA.* 110:1416–1421. http://dx.doi.org/10.1073/pnas.1213480110

Cronin, S.J., and J.M. Penninger. 2007. From T-cell activation signals to signaling control of anti-cancer immunity. *Immunol. Rev.* 220:151–168. http://dx.doi.org/10.1111/j.1600-065X.2007.00570.x

Doh, J., and M.F. Krummel. 2010. Immunological synapses within context: patterns of cell-cell communication and their application in T-T interactions. *Curr. Top. Microbiol. Immunol.* 340:25–50.

Eickhoff, S., A. Brewitz, M.Y. Gerner, F. Klauschen, K. Komander, H. Hemmi, N. Garbi, T. Kaisho, R.N. Germain, and W. Kastenmüller. 2015. Robust Anti-viral Immunity Requires Multiple Distinct T Cell-Dendritic Cell Interactions. *Cell.* 162:1322–1337. http://dx.doi.org/10.1016/j.cell.2015.08.004

Fabbri, M., S. Di Meglio, M.C. Gagliani, E. Consonni, R. Molteni, J.R. Bender, C. Tacchetti, and R. Pardi. 2005. Dynamic partitioning into lipid rafts controls the endo-exocytic cycle of the alphaL/beta2 integrin, LFA-1, during leukocyte chemotaxis. *Mol. Biol. Cell.* 16:5793–5803. http://dx.doi.org/10.1091/mbc.E05-05-0413

Gérard, A., O. Khan, P. Beemiller, E. Oswald, J. Hu, M. Matloubian, and M.F. Krummel. 2013. Secondary T cell-T cell synaptic interactions drive the differentiation of protective CD8+ T cells. *Nat. Immunol.* 14:356–363. http://dx.doi.org/10.1038/ni.2547

Ghosh, S., A.A. Chackerian, C.M. Parker, C.M. Ballantyne, and S.M. Behar. 2006. The LFA-1 adhesion molecule is required for protective immunity during pulmonary Mycobacterium tuberculosis infection. *J. Immunol.* 176:4914–4922. http://dx.doi.org/10.4049/jimmunol.176.8.4914

Graf, B., T. Bushnell, and J. Miller. 2007. LFA-1-mediated T cell costimulation through increased localization of TCR/class II complexes to the central supramolecular activation cluster and exclusion of CD45 from the immunological synapse. *J. Immunol.* 179:1616–1624. http://dx.doi.org/10.4049/jimmunol.179.3.1616

Graham, J.M. 2002. Separation of membrane vesicles and cytosol from cultured cells and bacteria in a preformed discontinuous gradient. *Sci. World J.* 2:1555–1559. http://dx.doi.org/10.1100/tsw.2002.834

Haddad, E.K., X. Wu, J.A. Hammer III, and P.A. Henkart. 2001. Defective granule exocytosis in Rab27a-deficient lymphocytes from Ashen mice. *J. Cell Biol.* 152:835–842. http://dx.doi.org/10.1083/jcb.152.4.835

Hogg, N., I. Patzak, and F. Willenbrock. 2011. The insider's guide to leukocyte integrin signalling and function. *Nat. Rev. Immunol.* 11:416–426. http://dx.doi.org/10.1038/nri2986

Hosseini, B.H., I. Louban, D. Djandji, G.H. Wabnitz, J. Deeg, N. Bulbuc, Y. Samstag, M. Gunzer, J.P. Spatz, and G.J. Hämmerling. 2009. Immune synapse formation determines interaction forces between T cells and antigen-presenting cells measured by atomic force microscopy. *Proc. Natl. Acad. Sci. USA.* 106:17852–17857. (published erratum appears in *Proc. Natl. Acad. Sci. USA.* 2010. 107:2373) http://dx.doi.org/10.1073/pnas.0905384106

Hyun, Y.M., H.L. Chung, J.L. McGrath, R.E. Waugh, and M. Kim. 2009. Activated integrin VLA-4 localizes to the lamellipodia and mediates T cell migration on VCAM-1. *J. Immunol.* 183:359–369. http://dx.doi.org/10.4049/jimmunol.0803388

Hyun, Y.M., R. Sumagin, P.P. Sarangi, E. Lomakina, M.G. Overstreet, C.M. Baker, D.J. Fowell, R.E. Waugh, I.H. Sarelius, and M. Kim. 2012. Uropod elongation is a common final step in leukocyte extravasation through inflamed vessels. *J. Exp. Med.* 209:1349–1362. http://dx.doi.org/10.1084/jem.20111426

Kaech, S.M., E.J. Wherry, and R. Ahmed. 2002. Effector and memory T-cell differentiation: implications for vaccine development. *Nat. Rev. Immunol.* 2:251–262. http://dx.doi.org/10.1038/nri778

Kandula, S., and C. Abraham. 2004. LFA-1 on CD4+ T cells is required for optimal antigen-dependent activation in vivo. *J. Immunol.* 173:4443–4451. http://dx.doi.org/10.4049/jimmunol.173.7.4443

Katakai, T., K. Habiro, and T. Kinashi. 2013. Dendritic cells regulate high-speed interstitial T cell migration in the lymph node via LFA-1/ICAM-1. *J. Immunol.* 191:1188–1199. http://dx.doi.org/10.4049/jimmunol.1300739

Kelso, A., E.O. Costelloe, B.J. Johnson, P. Groves, K. Buttigieg, and D.R. Fitzpatrick. 2002. The genes for perforin, granzymes A-C and IFN-gamma are differentially expressed in single CD8(+) T cells during primary activation. *Int. Immunol.* 14:605–613. http://dx.doi.org/10.1093/intimm/dxf028

Kim, M., C.V. Carman, and T.A. Springer. 2003. Bidirectional transmembrane signaling by cytoplasmic domain separation in integrins. *Science.* 301:1720–1725. http://dx.doi.org/10.1126/science.1084174

Kim, M., C.V. Carman, W. Yang, A. Salas, and T.A. Springer. 2004. The primacy of affinity over clustering in regulation of adhesiveness of the integrin alphaLbeta2. *J. Cell Biol.* 167:1241–1253. http://dx.doi.org/10.1083/jcb.200404160

Kinashi, T., and K. Katagiri. 2004. Regulation of lymphocyte adhesion and migration by the small GTPase Rap1 and its effector molecule, RAPL. *Immunol. Lett.* 93:1–5. http://dx.doi.org/10.1016/j.imlet.2004.02.008

King, C.G., S. Koehli, B. Hausmann, M. Schmaler, D. Zehn, and E. Palmer. 2012. T cell affinity regulates asymmetric division, effector cell differentiation, and tissue pathology. *Immunity.* 37:709–720. http://dx.doi.org/10.1016/j.immuni.2012.06.021

Koniaras, C., F.R. Carbone, W.R. Heath, and A.M. Lew. 1999. Inhibition of naïve class I-restricted T cells by altered peptide ligands. *Immunol. Cell Biol.* 77:318–323. http://dx.doi.org/10.1046/j.1440-1711.1999.00828.x

Macia, E., M. Ehrlich, R. Massol, E. Boucrot, C. Brunner, and T. Kirchhausen. 2006. Dynasore, a cell-permeable inhibitor of dynamin. *Dev. Cell.* 10:839–850. http://dx.doi.org/10.1016/j.devcel.2006.04.002

Matloubian, M., C.G. Lo, G. Cinamon, M.J. Lesneski, Y. Xu, V. Brinkmann, M.L. Allende, R.L. Proia, and J.G. Cyster. 2004. Lymphocyte egress from thymus and peripheral lymphoid organs is dependent on S1P receptor 1. *Nature.* 427:355–360. http://dx.doi.org/10.1038/nature02284

Matsumoto, G., E. Kubota, Y. Omi, U. Lee, and J.M. Penninger. 2004. Essential role of LFA-1 in activating Th2-like responses by alpha-galactosylceramide-activated NKT cells. *J. Immunol.* 173:4976–4984. http://dx.doi.org/10.4049/jimmunol.173.8.4976

Mempel, T.R., S.E. Henrickson, and U.H. Von Andrian. 2004. T-cell priming by dendritic cells in lymph nodes occurs in three distinct phases. *Nature.* 427:154–159. http://dx.doi.org/10.1038/nature02238

Ni, H.T., M.J. Deeths, and M.F. Mescher. 2001. LFA-1-mediated costimulation of CD8+ T cell proliferation requires phosphatidylinositol 3-kinase activity. *J. Immunol.* 166:6523–6529. http://dx.doi.org/10.4049/jimmunol.166.11.6523

Nishikimi, A., S. Ishihara, M. Ozawa, K. Etoh, M. Fukuda, T. Kinashi, and K. Katagiri. 2014. Rab13 acts downstream of the kinase Mst1 to deliver the integrin LFA-1 to the cell surface for lymphocyte trafficking. *Sci. Signal.* 7:ra72. http://dx.doi.org/10.1126/scisignal.2005199

Parameswaran, N., R. Suresh, V. Bal, S. Rath, and A. George. 2005. Lack of ICAM-1 on APCs during T cell priming leads to poor generation of central memory cells. *J. Immunol.* 175:2201–2211. http://dx.doi.org/10.4049/jimmunol.175.4.2201

Pham, T.H., T. Okada, M. Matloubian, C.G. Lo, and J.G. Cyster. 2008. S1P1 receptor signaling overrides retention mediated by G alpha i-coupled receptors to promote T cell egress. *Immunity.* 28:122–133. http://dx.doi.org/10.1016/j.immuni.2007.11.017

Reichardt, P., I. Patzak, K. Jones, E. Etemire, M. Gunzer, and N. Hogg. 2013. A role for LFA-1 in delaying T-lymphocyte egress from lymph nodes. *EMBO J.* 32:829–843. http://dx.doi.org/10.1038/emboj.2013.33

Salomon, B., and J.A. Bluestone. 1998. LFA-1 interaction with ICAM-1 and ICAM-2 regulates Th2 cytokine production. *J. Immunol.* 161:5138–5142.

Scholer, A., S. Hugues, A. Boissonnas, L. Fetler, and S. Amigorena. 2008. Intercellular adhesion molecule-1-dependent stable interactions between T cells and dendritic cells determine CD8+ T cell memory. *Immunity.* 28:258–270. http://dx.doi.org/10.1016/j.immuni.2007.12.016

Shulman, Z., V. Shinder, E. Klein, V. Grabovsky, O. Yeger, E. Geron, A. Montresor, M. Bolomini-Vittori, S.W. Feigelson, T. Kirchhausen, et al. 2009. Lymphocyte crawling and transendothelial migration require chemokine triggering of high-affinity LFA-1 integrin. *Immunity.* 30:384–396. http://dx.doi.org/10.1016/j.immuni.2008.12.020

Smith, A., M. Bracke, B. Leitinger, J.C. Porter, and N. Hogg. 2003. LFA-1-induced T cell migration on ICAM-1 involves regulation of MLCK-mediated attachment and ROCK-dependent detachment. *J. Cell Sci.* 116:3123–3133. http://dx.doi.org/10.1242/jcs.00606

Smith, A., P. Stanley, K. Jones, L. Svensson, A. McDowall, and N. Hogg. 2007. The role of the integrin LFA-1 in T-lymphocyte migration. *Immunol. Rev.* 218:135–146. http://dx.doi.org/10.1111/j.1600-065X.2007.00537.x

Stanley, P., S. Tooze, and N. Hogg. 2012. A role for Rap2 in recycling the extended conformation of LFA-1 during T cell migration. *Biol. Open.* 1:1161–1168. http://dx.doi.org/10.1242/bio.20122824

Stinchcombe, J.C., D.C. Barral, E.H. Mules, S. Booth, A.N. Hume, L.M. Machesky, M.C. Seabra, and G.M. Griffiths. 2001. Rab27a is required for regulated secretion in cytotoxic T lymphocytes. *J. Cell Biol.* 152:825–834. http://dx.doi.org/10.1083/jcb.152.4.825

Svensson, L., P. Stanley, F. Willenbrock, and N. Hogg. 2012. The Gαq/11 proteins contribute to T lymphocyte migration by promoting turnover of integrin LFA-1 through recycling. *PLoS One.* 7:e38517. http://dx.doi.org/10.1371/journal.pone.0038517

Van Seventer, G.A., Y. Shimizu, K.J. Horgan, and S. Shaw. 1990. The LFA-1 ligand ICAM-1 provides an important costimulatory signal for T cell receptor-mediated activation of resting T cells. *J. Immunol.* 144:4579–4586.

Varga, G., N. Nippe, S. Balkow, T. Peters, M.K. Wild, S. Seeliger, S. Beissert, M. Krummen, J. Roth, C. Sunderkötter, and S. Grabbe. 2010. LFA-1 contributes to signal I of T-cell activation and to the production of T(h)1 cytokines. *J. Invest. Dermatol.* 130:1005–1012. http://dx.doi.org/10.1038/jid.2009.398

von Andrian, U.H., and C.R. Mackay. 2000. T-cell function and migration. Two sides of the same coin. *N. Engl. J. Med.* 343:1020–1034. http://dx.doi.org/10.1056/NEJM200010053431407

Wang, Y., D. Li, R. Nurieva, J. Yang, M. Sen, R. Carreño, S. Lu, B.W. McIntyre, J.J. Molldrem, G.B. Legge, and Q. Ma. 2009. LFA-1 affinity regulation is necessary for the activation and proliferation of naive T cells. *J. Biol. Chem.* 284:12645–12653. http://dx.doi.org/10.1074/jbc.M807207200

Weber, K.S., C. Weber, G. Ostermann, H. Dierks, W. Nagel, and W. Kolanus. 2001. Cytohesin-1 is a dynamic regulator of distinct LFA-1 functions in leukocyte arrest and transmigration triggered by chemokines. *Curr. Biol.* 11:1969–1974. http://dx.doi.org/10.1016/S0960-9822(01)00597-8

Woolf, E., I. Grigorova, A. Sagiv, V. Grabovsky, S.W. Feigelson, Z. Shulman, T. Hartmann, M. Sixt, J.G. Cyster, and R. Alon. 2007. Lymph node chemokines promote sustained T lymphocyte motility without triggering stable integrin adhesiveness in the absence of shear forces. *Nat. Immunol.* 8:1076–1085. http://dx.doi.org/10.1038/ni1499

Xin, A., F. Masson, Y. Liao, S. Preston, T. Guan, R. Gloury, M. Olshansky, J.X. Lin, P. Li, T.P. Speed, et al. 2016. A molecular threshold for effector CD8(+) T cell differentiation controlled by transcription factors Blimp-1 and T-bet. *Nat. Immunol.* 17:422–432. http://dx.doi.org/10.1038/ni.3410

Yeo, C.J., and D.T. Fearon. 2011. T-bet-mediated differentiation of the activated CD8+ T cell. *Eur. J. Immunol.* 41:60–66. http://dx.doi.org/10.1002/eji.201040873

Zumwalde, N.A., E. Domae, M.F. Mescher, and Y. Shimizu. 2013. ICAM-1-dependent homotypic aggregates regulate CD8 T cell effector function and differentiation during T cell activation. *J. Immunol.* 191:3681–3693. http://dx.doi.org/10.4049/jimmunol.1201954